

Electrochemical preparation of TiO₂/SiO₂ composite film and its high activity toward the photoelectrocatalytic degradation of methyl orange

Zhixiong Zhou · Lihua Zhu · Jing Li ·
Heqing Tang

Received: 17 August 2008 / Accepted: 6 March 2009 / Published online: 18 March 2009
© Springer Science+Business Media B.V. 2009

Abstract Uniform TiO₂/SiO₂ composite films were prepared on ITO substrates by electrodeposition, and highly photoelectrocatalytic (PEC) activity of the composite films was observed toward the degradation of methyl orange (MO) in aqueous solutions. It was further found that their PEC activity was dependent on the electrodeposition parameters including deposition time, solution pH and SiO₂ content. Under the optimized condition, the PEC degradation of MO on TiO₂/SiO₂ composite film electrode could be enhanced about 14 times relative to that on neat TiO₂ film electrode. The high PEC activity of the TiO₂/SiO₂ composite film electrode was mainly attributed to the enhancement of the charge separation of photo-generated electron-hole pairs by the dispersion of SiO₂ nanoparticles in the TiO₂ matrix with the aid of the applied electric field.

Keywords Photoelectrocatalysis · Electrodeposition · Titanium dioxide · Silicon dioxide

1 Introduction

Recently, photoelectrocatalytic (PEC) technologies have been studied extensively [1–5]. One of the earlier reports about the PEC application of TiO₂ films is the work of Vinodgopal et al., who prepared TiO₂ films and degraded 4-chlorophenol over the TiO₂ film electrode by an

electrochemically assisted photocatalytic method [6]. To improve the PEC activity of TiO₂ electrodes, we may adopt the following methods: controlling the morphology and surface structure of TiO₂ films [7], combining the PEC process with other reactions [8, 9], and doping the TiO₂ films with other metallic and non-metallic elements [10–13]. For example, Quan and coworkers reported that the TiO₂ nanotube electrode increased the PEC degradation of pentachlorophenol by 86.5%, relative to common TiO₂ film electrode [7]; the introduction of Fenton process was found to increase the PEC degradation rate of 2, 4, 6-trichlorophenol on TiO₂ by 2.3 times [8]; Yang et al. observed that the ZnO/TiO₂ films could increase about 25% in the PEC activity relative to the neat TiO₂ film [13].

We are interested in the effects of SiO₂ on the PC and PEC activity of TiO₂ films. The addition of SiO₂ in TiO₂ nanoparticle photocatalysts is able to increase the surface acidity [10], to increase the active surface area [14], to promote the adsorption of organic compounds [15], to help the electron transfer [16], and to modify the band gap [17], leading to enhanced PC decomposition of organic pollutants [18–20]. It is possible to increase the PC and PEC activity of TiO₂ films by introducing SiO₂ into the film.

TiO₂ thin films have been prepared through various methods, such as sputtering [21], chemical vapor deposition [22], spray pyrolysis [23], sol-gel [24], electrophoresis [25] and electrodeposition [26, 27]. Fukuda used an electrophoretic process to prepare TiO₂/SiO₂ composite film from a suspension of TiO₂ and SiO₂ particles [25]. Peiró et al. reported that TiO₂ nanoparticles are stable in Ti precursor solution for more than 10 h [28], and we also found that SiO₂ nanoparticles were stable in Ti precursor solution in our preliminary work. Therefore, we tried to prepare uniform TiO₂/SiO₂ composite films from SiO₂-suspended Ti precursor solution through a hybrid method

Z. Zhou · L. Zhu (✉) · J. Li · H. Tang (✉)
College of Chemistry and Chemical Engineering, Huazhong
University of Science and Technology, Wuhan 430074,
People's Republic of China
e-mail: lh Zhu63@yahoo.com.cn

H. Tang
e-mail: hqtang62@yahoo.com.cn

by combining electrodeposition with electrophoresis in the present work. The prepared composite films were confirmed to show high PEC efficiency in the degradation of methyl orange (MO) as a model organic pollutant.

2 Experimental

2.1 Materials and reagents

Indium-doped tin oxide (ITO) coated glass from obtained from Matsuta Vacuum Co., Ltd (Japan). SiO₂ nanoparticles (SP1) were provided by Zhoushan Nano Company (China). Tetrabutyl titanate (chemical grade, $\geq 85\%$) and other chemicals (analytical grade, $\geq 99\%$) were obtained from Chengdu Kelong Chemical Reagent Company (China), and used as received. Distilled water was used throughout the present work.

2.2 Preparation of the suspension for electrodeposition

To prepare the suspensions for the electrodeposition, SiO₂ nanoparticles (0.06 g, 1 mmol) were dispersed in 25 mL of H₂O and 360 μL of HNO₃ (65 wt%) with ultrasonication for 5 min, and tetrabutyl titanate (0.679 g, 2 mmol) was dissolved in a mixture of 25 mL of EtOH and 300 μL of H₂O₂ (30 wt%). The solution of tetrabutyl titanate was added dropwise to the suspension of SiO₂, and the resulting suspension was homogenized by ultrasonication for 5 min.

2.3 Electrochemical preparation of TiO₂/SiO₂ composite films

All electrodeposition processes were carried out in an open one-compartment cell of 80 mL capacity filled with 50 mL of the prepared suspension mentioned above. After the ITO glass was ultrasonically washed in 0.1 mol L⁻¹ HNO₃, EtOH, and then distilled water, the ITO electrode (2 × 2.5 cm) was used as the cathode, being 1 cm distant from a Pt foil (10 cm²) as the anode. The bias was controlled at 2 V constantly by using a CHI440 electrochemical analyzer system (CH Instruments). After being cleaned with distilled water, the deposited film was dried under the atmospheric ambient and then calcined at 450 °C for 2 h, unless specified elsewhere.

2.4 Characterization

The surface morphology was examined on a FEI Sirion-200 scanning electron microscope (SEM) and a Sounding Housing SPA 400 atomic force microscope (AFM). X-ray diffraction (XRD) was performed on a diffractometer (PANalytical B-V. X'Pert PRO). XPS spectra were recorded

by using a XSAM 800 spectrometer (Kratos Ltd. In England) working in the FRR mode with Mg K α radiation as the excitation source. The binding energy (BE) reference was taken at the C 1s at 284.2 eV.

2.5 PEC experiment

PEC experiments were carried out in a cylindrical glass cell with a 9 W UV lamp (Philips, $\lambda_{\text{max}} = 253.7$ nm) as the light source, being set in a quartz tube immersed into solution. The film electrodes with a total working area of 5 cm⁻² were all placed in 200 mL solution of 10 mg L⁻¹ MO + 0.1 mol L⁻¹ NaCl, and the distance from the working surface of the film electrode to the UV lamp was kept at 2 cm. The initial pH of solution was 2.7 unless specified elsewhere. The composite film electrode, a Pt foil (10 cm²) and a saturated calomel electrode (SCE) were used as the anode, cathode and reference electrode, respectively. The electrode potential of all PEC experiments was kept at 0.8 V (vs. SCE) unless specified elsewhere. The solution was maintained under magnetic stirring during the PEC experiment. At given time intervals, aliquots (2 mL) of the solution were sampled, and the remained MO concentration was determined by measuring the absorbance of MO at its maximum absorption wavelength of 515 nm on a UV-visible spectrophotometer (Varian). At least triplicate runs were carried out for each test, and the standard deviation was generally less than 5%. For a comparison, the EC and PC experiments were carried out similarly but without the light irradiation or without the application of electrode potential.

3 Results and discussion

3.1 The preparation and characterization of TiO₂/SiO₂ composite films

A high quality of TiO₂/SiO₂ composite film requires a uniform dispersion of SiO₂ particles in the TiO₂ matrix. Thus, the preparation of stable SiO₂-dispersed Ti precursor suspensions is critical to make the SiO₂ particles distribute uniformly in the TiO₂ matrix. The stability of the SiO₂ suspension is attributable to the surface charge of the SiO₂ nanoparticles dispersed in the solution, which can be effectively achieved by adding a small amount of concentrated HNO₃ to the dispersion. The nano-particles of SiO₂ become positively charged at pH 1.5 due to its low PZC of 2 [29]. The addition of H₂O₂ into the solution of tetrabutyl titanate in EtOH will result in a yellow solution due to the formation of peroxotitanium complexes, which prevent the condensation of Ti cations. The peroxotitanium complexes are also positively charged [30] in the

electrolytic suspension at pH 1.5. Therefore, the prepared SiO_2 -dispersed Ti precursor suspensions were observed to be stable.

The deposition of $\text{TiO}_2/\text{SiO}_2$ film in the present work is an electrochemical co-deposition process. When no any SiO_2 particles are present in the aqueous solution of Ti precursor, titanium hydroxide ($\text{TiO}_3(\text{H}_2\text{O})_x$) will be electrochemically deposited onto the surface of the ITO cathode because of the surface alkalization arising from the hydrogen evolution [28]. At a bias of 2.0 V, the positively charged peroxotitanium complexes are transported to the vicinity of the cathode, where the solution is basic due to the presence of electrogenerated OH^- ions. Then it may cause the precipitation of an insoluble peroxotitanium hydrate, $\text{TiO}_3(\text{H}_2\text{O})_x$ ($1 < x < 2$) [31]. In addition, the positively charged SiO_2 nanoparticles are also electrophoretically transported toward the cathode, and co-deposited with the above mentioned peroxotitanium hydrate. As expected, uniform, compact and adherent composite films were easily obtained; this was confirmed by examination of the morphology of the TiO_2 films and $\text{TiO}_2/\text{SiO}_2$ composite films as shown in Fig. 1. Possibly due to hydrogen evolution during the electrodeposition, nano-pores (or pits) were observed on the surface of the electrodeposited TiO_2 film (Fig. 1a). The $\text{TiO}_2/\text{SiO}_2$ composite film also had such a porous structure and exhibited a roughly uniform distribution of SiO_2 particles in the continuous TiO_2 substrate (Fig. 1b). The surface morphology of the films was also observed with AFM. As shown in Fig. 2, the images indicated that the $\text{TiO}_2/\text{SiO}_2$ composite film has a slightly rougher surface than the TiO_2 film, suggesting that the $\text{TiO}_2/\text{SiO}_2$ composite film may have a greater real surface area, which is favorable to its PEC ability.

The co-deposition of SiO_2 and TiO_2 was further confirmed by the XRD measurements of the composite films. In order to eliminate the interference of the ITO substrate, we similarly prepared the films on the substrate of Ti, and obtained the XRD pattern of the composite film (Fig. 3). In

comparison with the XRD patterns of the single SiO_2 film, TiO_2 film and the Ti substrate, the presence of TiO_2 was clearly seen due to the appearance of all the diffraction peaks of TiO_2 , and the small peak at $2\theta = 22^\circ$ revealing that SiO_2 was imbedded into the composite film. Although the deposition process may be influenced by the deposition substrate, the imbedding of SiO_2 into the composited film deposited on Ti plate should also imply the imbedding of SiO_2 into the composited film deposited on ITO.

XPS spectra of the TiO_2 and $\text{TiO}_2/\text{SiO}_2$ films were recorded, and the envelopes Ti 2p, O 1s and Si 2p are shown in Fig. 4. The Ti $2p_{3/2}$ band was observed at binding energies of 464.0 and 458.9 eV for the TiO_2 and $\text{TiO}_2/\text{SiO}_2$ films respectively, while the Ti $2p_{1/2}$ band occurred at 469.7 eV for the TiO_2 film and 464.6 eV for the $\text{TiO}_2/\text{SiO}_2$ film (Fig. 4a). The shift (about -5 eV) in the binding energy of the Ti 2p bands is possibly related to the varied chemical environment of Ti arising from the embedding of SiO_2 into the TiO_2 matrix. This observation is consistent with that reported by Lassaletta et al. [32], who attributed such changes to a decrease in the positive charge on Ti atoms in the initial state due to the formation of mixed Ti–O–Si bonds at the interface of $\text{TiO}_2/\text{SiO}_2$. The O 1s band appeared at 530.3 eV for the TiO_2 film and 530.5 eV for the $\text{TiO}_2/\text{SiO}_2$ film (Fig. 4b), which is attributable to the Ti–O–Ti components (529.2 eV) [33]. The weak band at 103.4 eV was attributed to Si 2p (Fig. 4c), which, along with the chemical shift of Ti 2p induced by Si, further supported that SiO_2 was embedded in the TiO_2 matrix for the $\text{TiO}_2/\text{SiO}_2$ film.

3.2 Photocatalytic, electrocatalytic and photoelectrocatalytic activity of $\text{TiO}_2/\text{SiO}_2$ films

To evaluate the PEC activity of the prepared TiO_2 and $\text{TiO}_2/\text{SiO}_2$ films, the photocurrents on the film electrodes were first recorded in a solution of $10 \text{ mg L}^{-1} \text{MO} + 0.1 \text{ mol L}^{-1}$

Fig. 1 SEM images of the electrodeposited **a** TiO_2 film and **b** $\text{TiO}_2/\text{SiO}_2$ film ($\text{Si/Ti} = 1:2$)

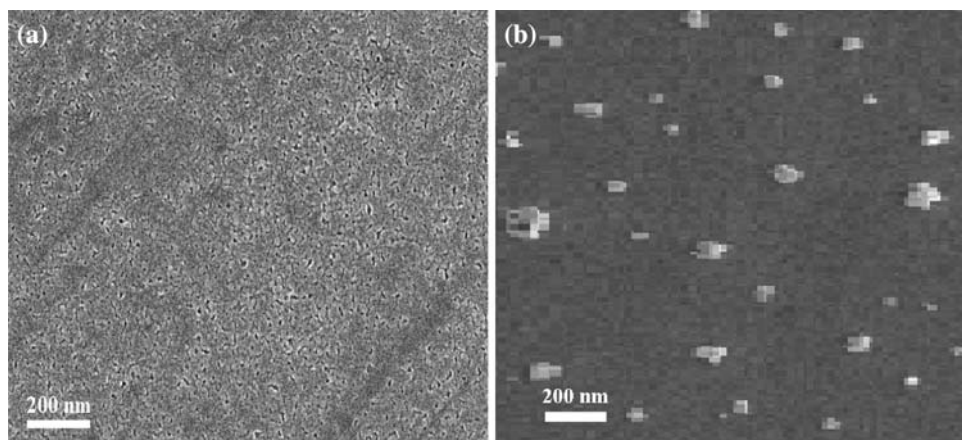


Fig. 2 AFM images of the electrodeposited **a** TiO₂ film and **b** TiO₂/SiO₂ film (Si/Ti = 1:2)

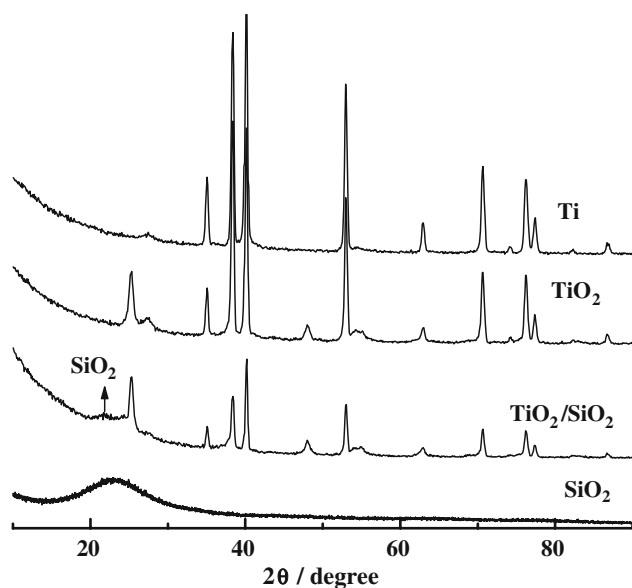
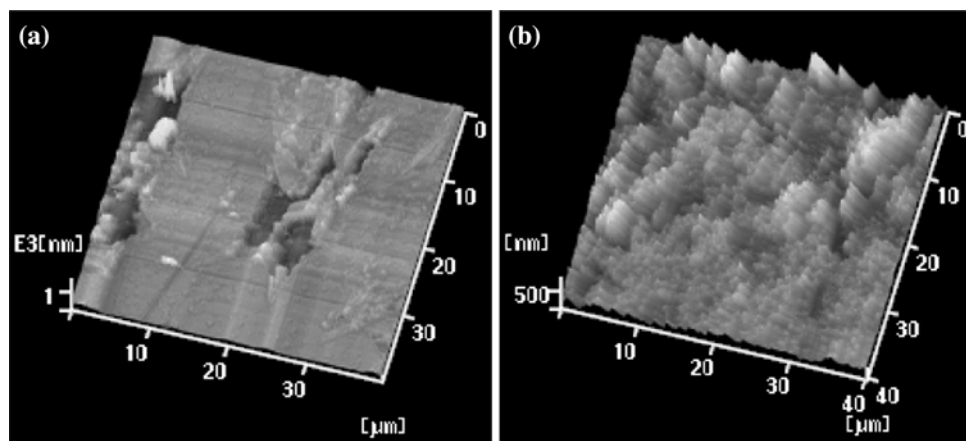


Fig. 3 XRD patterns of the SiO₂, Ti, TiO₂/Ti, and TiO₂/SiO₂/Ti (Si/Ti = 1:2) structures

NaCl at pH 2.7. As seen in Fig. 5, the photocurrent on the neat TiO₂ film electrode was about 0.18 mA, whereas the TiO₂/SiO₂ composite film (prepared with a Ti/Si ratio of 2:1) yielded a spiked photocurrent as high as about 1.2 mA, which approached an almost constant value of about 1.0 mA after the light was switched on. That is, the TiO₂/SiO₂ composite film showed a steady-state photocurrent 7 times higher than the neat TiO₂ film. Relative to the PC degradation of MO, the enhanced PEC degradation of MO on both the neat TiO₂ and composite films was consistent with the open-circuit potential shift when the light was switched on and off. The open-circuit potential of the TiO₂ and TiO₂/SiO₂ film electrodes were observed to be shifted from 0.41 and 0.46 V under the dark to −0.29 and −0.28 V under the UV illumination, respectively.

The direct photolysis, EC, PC and PEC processes of MO degradation were performed on the TiO₂/SiO₂ composite

film electrode in aqueous solutions as shown in Fig. 6. All these processes of MO degradation were found to behave as a pseudo first order reaction. The EC degradation of MO was slowest, showing an apparent rate constant (k_{EC}) of $0.6 \times 10^{-3} \text{ min}^{-1}$. Due to the UV irradiation, the direct photolysis of MO was observable with an apparent rate constant (k_{DP}) of $1.8 \times 10^{-3} \text{ min}^{-1}$. The PC activity of the composite film was demonstrated by the slight increasing of the apparent rate constant (k_{PC}) to $3.0 \times 10^{-3} \text{ min}^{-1}$. The MO degradation was greatly enhanced in the PEC degradation process, generating the apparent rate constant (k_{PEC}) of $105.1 \times 10^{-3} \text{ min}^{-1}$. Relative to the PC (or EC) degradation, the PEC degradation was promoted significantly by a factor of 31 (or 175) times.

The excellent PEC activity of the composite film is attributed to the dispersion of SiO₂ nanoparticles in the TiO₂ matrix of the film. Tachikawa et al. [4] recently reported that the sites of SiO₂ particles may act as adsorption sites of organic pollutants to increase the concentration of organic pollutants near the catalytic TiO₂ sites. Anderson and Bard [16] demonstrated that the dispersed SiO₂ particles favor the charge separation of the photo-generated electron/hole pairs. It seems reasonable to consider that the numerous contacts of the TiO₂ and SiO₂ sites in the TiO₂/SiO₂ composite film may have similar effects and promote the PEC process on the film. However, we observed that the composite film provided rather poor PC activity and very poor EC activity toward the degradation of MO (Fig. 6). This indicates that the increasing effect of the dispersed SiO₂ nanoparticles is weak on the active area of the composite film and/or the adsorption of organic compounds on the surface of the film. There should be another important reason for the excellent PEC activity of the composite film. In consideration of the much increased photocurrent on the composite film electrode relative to the neat TiO₂ film electrode (Fig. 5) and the moderate PC activity of the composite film (curve 2 in Fig. 6), we believe that the SiO₂ dispersion in TiO₂ films

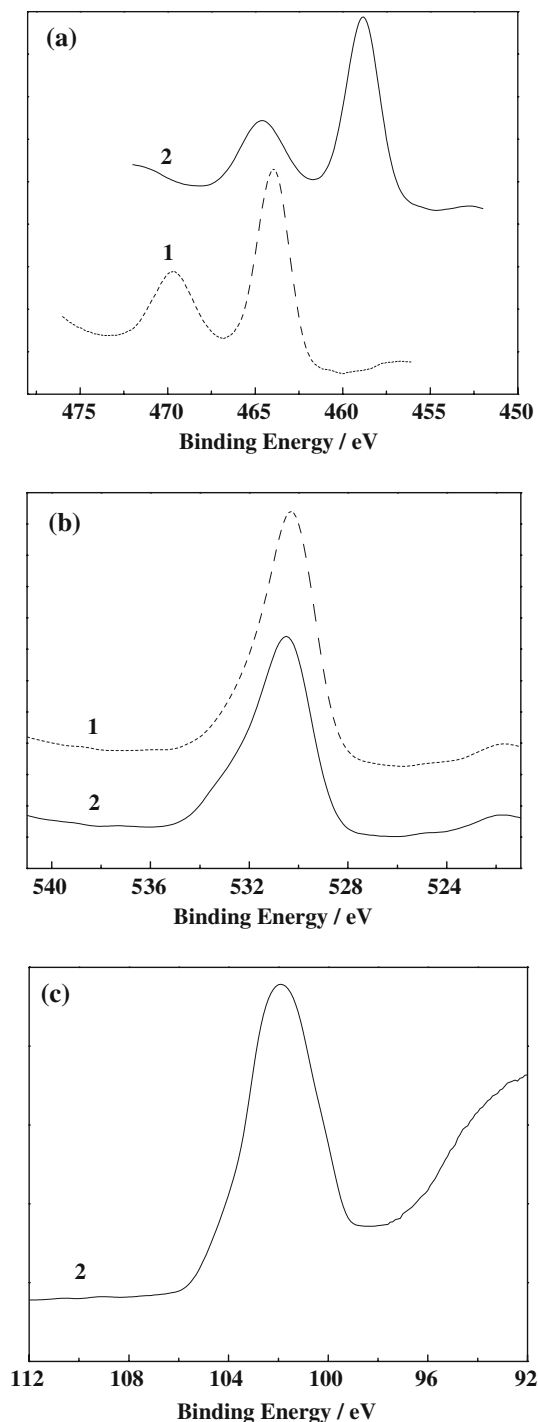


Fig. 4 XPS envelopes of **a** Ti 2p, **b** O 1s and **c** Si 2p for the TiO₂ (1) and TiO₂/SiO₂ (2) films

may enhance the separation of photo-generated e⁻-h⁺ pairs, which is supported by the work of Somasundaram and coworkers, who reported that the particle/matrix contacts aid in vectorial e⁻-h⁺ separation and charge transport [34]. As demonstrated by XPS analysis in the present work (Fig. 4) and Lassaletta et al. [32], Ti-O-Si bonds result in

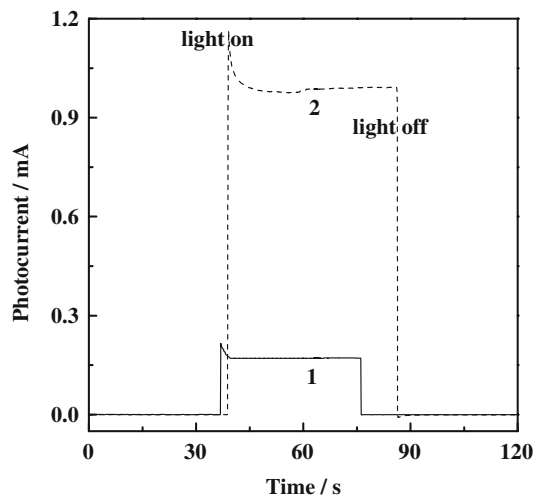


Fig. 5 Photocurrent recorded on (1) TiO₂ and (2) TiO₂/SiO₂ (Si/Ti = 1:2) film electrodes at 0.8 V in a solution of 10 mg L⁻¹ MO and 0.1 mol L⁻¹ NaCl at pH 2.7

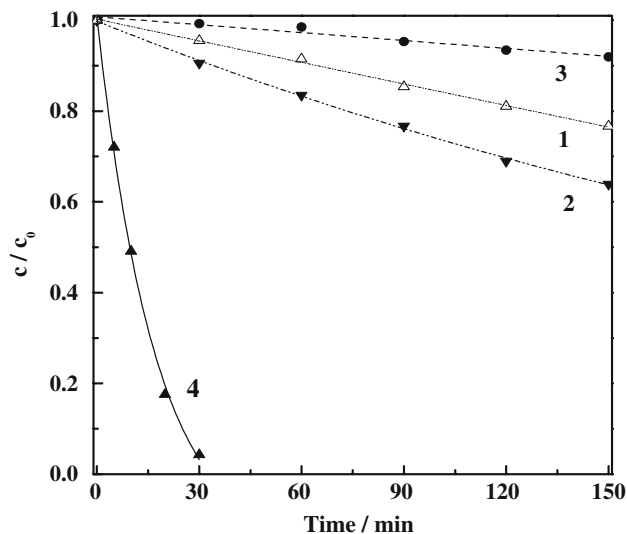


Fig. 6 Kinetics of the direct photolysis (1), PC (2), EC (3), and PEC (4) processes of MO degradation on TiO₂/SiO₂ (Si/Ti = 1:2) films. Both the EC and PEC degradation processes were carried out at a potential of 0.8 V

the formation TiO₂-SiO₂ interface at the particle/matrix contacts, leading to decreasing of the positive charge of the Ti atoms at the interface and the mobility of the electrons in the titania phase. If the electron transfer is not efficient, the charge separation of photo-generated e⁻-h⁺ pairs will be depressed due to the fast recombination of the photo-generated electrons and holes. Once the composite film electrode is applied with an appropriate electrode potential, the electron transfer is promoted, and the charge separation of the photo-generated e⁻-h⁺ pairs is much enhanced. This will result in an excellent activity under the combination of UV irradiation and the electrochemical oxidation.

3.3 Effects of reaction parameters on PEC activity of $\text{TiO}_2/\text{SiO}_2$ composite films

3.3.1 Effect of SiO_2 content in the preparation suspensions

We attempted to evaluate the effects of the SiO_2 content in the composite film on the PEC activity of the composite films, but we failed to get the exact SiO_2 content because the composite films were very thin and adhesive to the substrate and also because the absolute SiO_2 content was very small in the film. Instead of SiO_2 nanoparticles in the film, therefore, we used the content of that in the preparation suspensions to evaluate the effects of the SiO_2 content in the composite film on the PEC activity of the composite films, because the content of SiO_2 nanoparticles in the preparation suspensions would influence the SiO_2 content in the $\text{TiO}_2/\text{SiO}_2$ composite film, and then its PC, EC, and PEC activity.

The PC and EC activity of the SiO_2 -free TiO_2 film is compared with that of the $\text{TiO}_2/\text{SiO}_2$ composite film in Fig. 7.

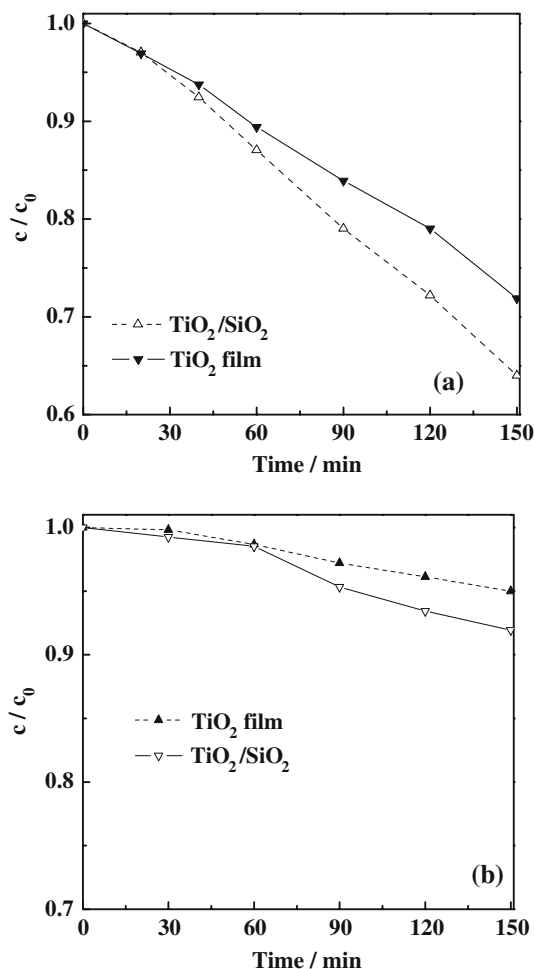


Fig. 7 Kinetics of **a** PC and **b** EC degradation of 10 mg L^{-1} MO in the presence of 0.1 mol L^{-1} NaCl at pH 2.7 on the TiO_2 and $\text{TiO}_2/\text{SiO}_2$ ($\text{Si/Ti} = 1:2$) film electrodes

The two films were not so different in their PC or EC activity, and the slightly better PC or EC activity of the $\text{TiO}_2/\text{SiO}_2$ film than the TiO_2 film was partly attributed the increased surface area of the and $\text{TiO}_2/\text{SiO}_2$ film (Fig. 2). However, the difference in the PEC activity is significant between the two films. The effects of the relative content of SiO_2 in the preparation suspensions are shown in Fig. 8 on the apparent rate constant and the photocurrent for the PEC degradation of MO on the $\text{TiO}_2/\text{SiO}_2$ composite films at 0.8 V. As the relative content of SiO_2 is increased, both the degradation photocurrent and the rate constant first increase and then decrease, showing an optimal value at the Si/Ti ratio of 1:2. The ratio of the PEC degradation rate constant for the $\text{TiO}_2/\text{SiO}_2$ films to that for the neat TiO_2 film achieves 13.9 when the Si/Ti ratio is 1:2. The initial increase of the PEC activity of the composite films with increasing Si/Ti ratio is attributable to the addition of SiO_2 nanoparticles into the TiO_2 film as discussed in Sect. 3.2. We also know that a pure SiO_2 film has no PEC activity. If the percentage of Si in the composite film (corresponding to a Si/Ti ratio in the preparation dispersion) is too high, the composite film will behave like a pure SiO_2 film with poor PEC performance. Thus, both the degradation photocurrent and the apparent rate constant decrease when $\text{Si/Ti} > 1/2$, as shown in Fig. 8.

3.3.2 Effects of electrodeposition time and calcination temperature

The electrodeposition time changes the thickness of the $\text{TiO}_2/\text{SiO}_2$ film and then influences its PEC performance. As shown in Fig. 9a, the PEC degradation of MO is

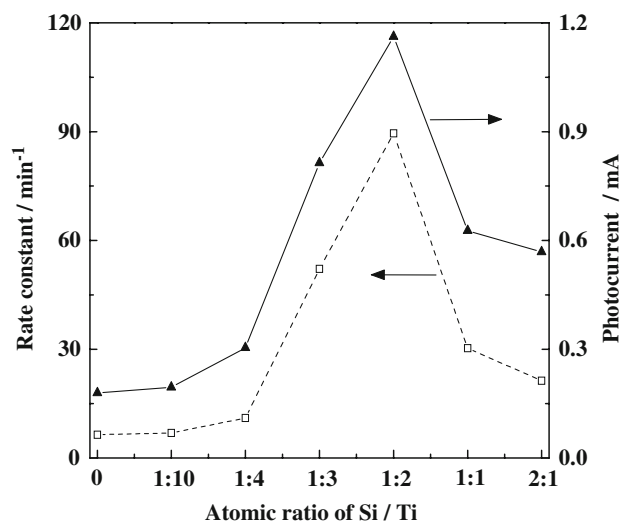


Fig. 8 Effects of the relative SiO_2 content in the preparation suspensions on the PEC degradation rate constant and photocurrent for the degradation of MO on the $\text{TiO}_2/\text{SiO}_2$ film electrodes prepared with a deposition time of 60 min

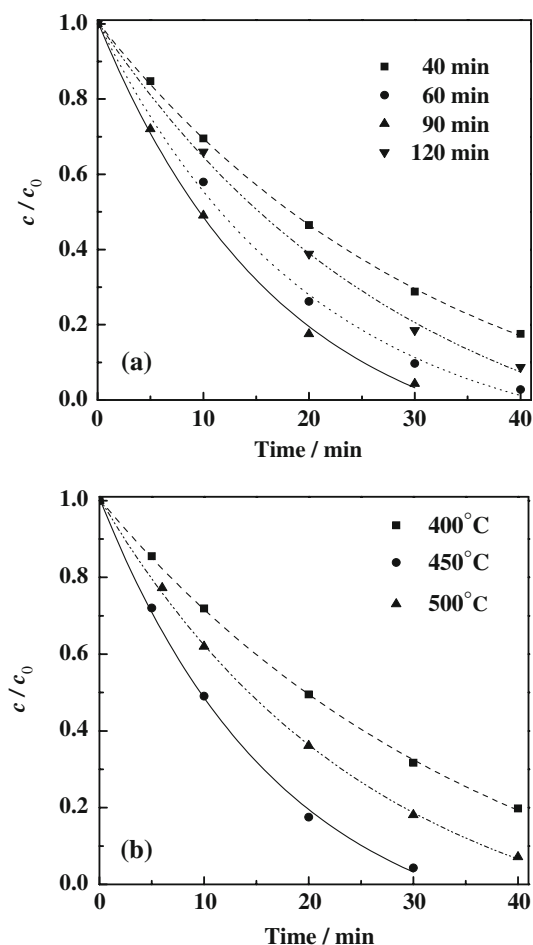


Fig. 9 Effects of the electrodeposition time (a) and calcination temperature (b) on the PEC degradation of MO on TiO₂/SiO₂ (Si/Ti = 1:2) film electrodes at 0.8 V in a solution of 10 mg L⁻¹ MO and 0.1 mol L⁻¹ NaCl at pH 2.7

enhanced with increase in electrodeposition time up to 90 min, and then decreases beyond 90 min. When the deposition time is less than 90 min, the amount of deposited TiO₂ (and SiO₂) increases with deposition time, and the greater amount of the deposit favors the PEC activity. However, an over-long time deposition will increase the TiO₂/SiO₂ deposits, leading to poorer electrical conductivity across the film. Therefore, the degradation decreases for deposition times beyond 90 min.

The calcination temperature also influences the PEC property of the composite film (Fig. 9b). The rate constant of the PEC degradation of MO is increased from $45 \times 10^{-3} \text{ min}^{-1}$ for films calcined at 400 °C to $105 \times 10^{-3} \text{ min}^{-1}$ at 450 °C, by more than two times, and then decreases to $65 \times 10^{-3} \text{ min}^{-1}$ at 500 °C. It is known that the calcination temperature can influence both the phase transformation and the crystal size of TiO₂, and then strongly influence the PC activity of TiO₂ catalyst prepared with a sol-gel process. In the present work, calcination at

moderately high temperatures favors the transformation of TiO₂ from the amorphous structure to the anatase structure, which is required for PC and PEC activity of TiO₂-based films. When the temperature is increased to 600–1,100 °C, transformation from anatase to rutile structure occurs [35], which is unfavorable to the PC and PEC activity of TiO₂-based films. The optimum calcination temperature was 450 °C, being considerably lower than 600 °C. This is possibly related to the occluded SiO₂ and the necessity of the structure of the TiO₂/SiO₂ networks.

3.3.3 Effects of solution pH and applied potential

The initial pH values of solutions may influence the process through the following routes: the semiconductor flat-band potential variation, adsorption of electroactive species, and photoelectrochemical oxidation of water and OH⁻ ions competing with other reactants being possibly formed as powerful oxidants on irradiation [36]. Moreover, pH also affects the state of the reactant in solution, which ultimately changes the electrostatic interaction between the reactant and the TiO₂ surface [37]. Due to the slight change in solution pH during the experiments, only the initial pH was adjusted at the beginning of the experiments. The pH dependence of the PEC degradation of MO is presented in Fig. 10a. The PEC degradation of MO is markedly increased with decrease in solution pH, which is similar to the observation for the PEC degradation of pentachlorophenol on the TiO₂ nanotubes electrode reported by Yang et al. [38]. The TiO₂-based film may be charged positively at pH < 6.8 and the adsorption of MO on the film electrode surface increases with decreasing pH [39, 40]. Moreover, the MO species in the anthraquinone structure dominate that in the azo structure at pH < 3.1. The anthraquinone structure produces intermediates which are easy to break down further, whereas the intermediates from the azo structure are mainly benzene derivatives, which are usually degraded slowly [39]. Hence, the PEC degradation of MO on the TiO₂/SiO₂ film electrode is promoted as the solution pH decreases.

As discussed above, the applied anodic potential on the TiO₂/SiO₂ film electrode produces a potential gradient inside the film that forces the photo-generated holes and electrons to move in opposite directions [40] and suppresses the recombination of the photo-generated holes and electrons. As the positive potential increases, the resulting gradient enhances the separation of hole-electron pairs, leading to markedly increased photocurrents and rate constants of the PEC degradation of MO (Fig. 10b). The enhancing effect of potential becomes less pronounced at much more positive potentials. When the potential is more positive than 0.8 V, increase of the rate constant becomes less apparent and the photocurrent tends to saturate.

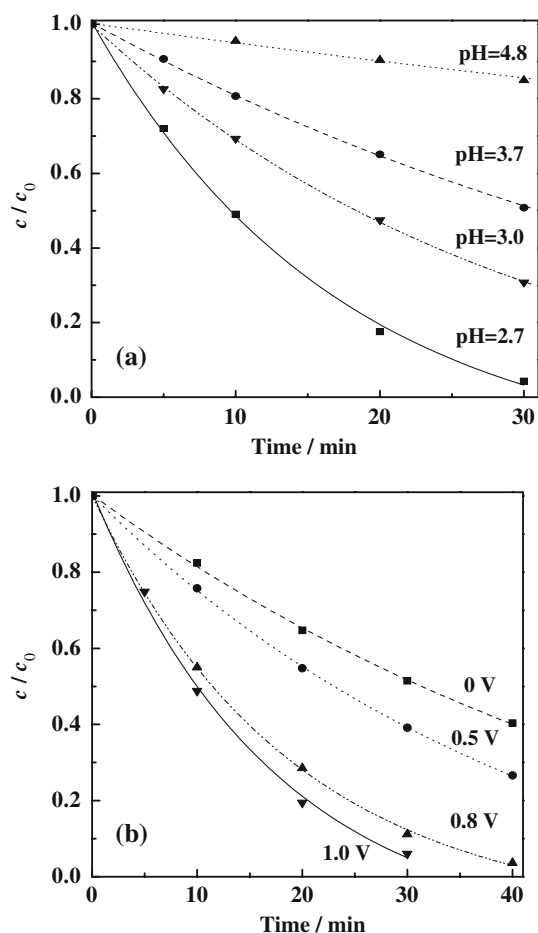


Fig. 10 Effects of initial solution pH (a) and applied electrode potential (b) on the PEC degradation of MO on $\text{TiO}_2/\text{SiO}_2$ ($\text{Si}/\text{Ti} = 1:2$) film electrodes at 0.8 V in a solution of 10 mg L^{-1} MO and 0.1 mol L^{-1} NaCl

3.4 Stability of $\text{TiO}_2/\text{SiO}_2$ composite film during repeated use in PEC experiments

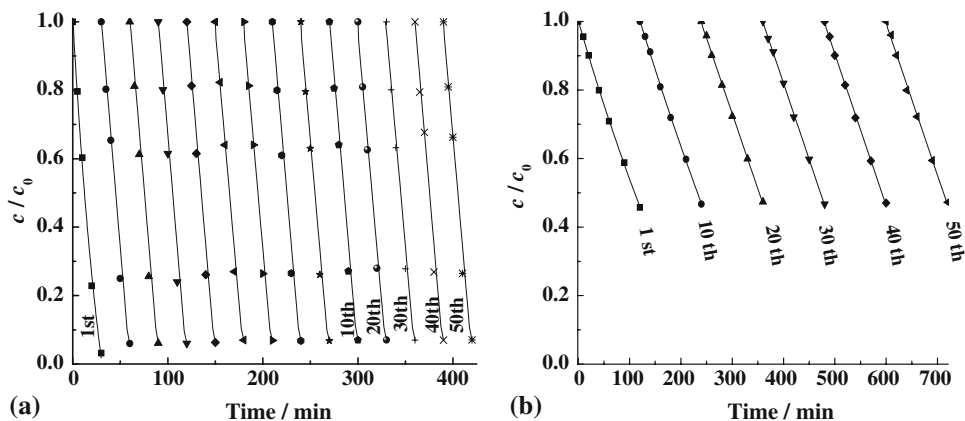
To evaluate the stability of the $\text{TiO}_2/\text{SiO}_2$ composite film as a PEC electrode, we carried out successively cycled

PEC degradation of MO at 0.8 V. As shown in Fig. 11, the PEC rate constants on both the $\text{TiO}_2/\text{SiO}_2$ composite film and the neat TiO_2 film electrodes are almost constant during the 50 runs, and that on the former is much greater than that on the latter ($k_{\text{composite}}/k_{\text{titania}} \approx 14$). This demonstrates that the composite film has good stability and duration for its application in the PEC degradation of organic pollutants, and confirms that the $\text{TiO}_2/\text{SiO}_2$ composite film electrode exhibits PEC activity which is much better than that of neat TiO_2 film.

4 Conclusions

Uniform and stable $\text{TiO}_2/\text{SiO}_2$ composite films were prepared on ITO glass via a modified electrodeposition method. The composite films had poor EC activity and moderate PC activity, but excellent PEC activity toward the degradation of MO. The greatly increased PEC activity of the $\text{TiO}_2/\text{SiO}_2$ composite film electrode is mainly due to the enhanced electron transfer and charge separation by the dispersed SiO_2 nanoparticles in the TiO_2 matrix. The preparation conditions were optimized at Si/Ti ratio of 1:2, electrodeposition time of 90 min, and annealing temperature of 450°C . The PEC degradation of MO on the composite film electrode could be further promoted by decreasing the solution pH to as low as 2.7 and applying an electrode potential as positive as 0.8 V. Under the optimized conditions, the PEC activity of the composite film was increased by about 14 times relative to the neat TiO_2 film. The effects of the reaction parameters on the PEC activity of the $\text{TiO}_2/\text{SiO}_2$ films were satisfactorily explained from the view point of the combined functions of the PE activity of TiO_2 and the enhancing effect of the dispersed SiO_2 on the charge separation of electron/hole pairs photo-induced in the domains of TiO_2 .

Fig. 11 Kinetics of successively cycled PEC degradation of MO on a $\text{TiO}_2/\text{SiO}_2$ and b TiO_2 film electrodes at 0.8 V in a solution of 10 mg L^{-1} MO and 0.1 mol L^{-1} NaCl at pH 2.7



Acknowledgments Funding is acknowledged from the National Natural Science Foundation of China (No. 2067709 and 30571536). The Analytical and Testing Center of Huazhong University of Science and Technology is thanked for its help in the characterization of the films.

References

1. Wu GS, Chen AC (2008) *J Photochem Photobiol A* 195:47
2. Shen XT, Zhu LH, Li J, Tang HQ (2007) *Chem Commun* 11:1163
3. Krysa J, Zlamal M, Waldner G (2007) *J Appl Electrochem* 37:1313
4. Tachikawa T, Fujitsuka M, Majima T (2007) *J Phys Chem C* 111:5259
5. Quan X, Ruan X, Zhao H, Chen S, Zhao Y (2007) *Environ Pollut* 147:409
6. Vinodgopal K, Hotchandani S, Kamat PV (1993) *J Phys Chem* 97:9040
7. Quan X, Yang S, Ruan X, Zhao H (2005) *Environ Sci Technol* 39:3770
8. Li XZ, Liu HS (2005) *Environ Sci Technol* 39:4614
9. Xie YB, Li XZ (2006) *Mater Chem Phys* 95:39
10. Guan K (2005) *Surf Coat Technol* 191:155
11. Egerton TA, Janus M, Morawski AW (2006) *Chemosphere* 63:1203
12. Nakamura R, Tanaka T, Nakato Y (2004) *J Phys Chem B* 108:10617
13. Yang S, Quan X, Li X, Liu Y, Chen S, Chen G (2004) *Phys Chem Chem Phys* 6:659
14. Marugán J, López-Muñoz MJ, Aguado J, van Grieken R (2007) *Catal Today* 124:103
15. Anderson C, Bard AJ (1997) *J Phys Chem B* 101:2611
16. Anderson C, Bard AJ (1995) *J Phys Chem* 99:9882
17. Aguado J, van Grieken R, López-Muñoz MJ, Marugán J (2006) *Appl Catal A* 312:202
18. Ruetten SA, Thomas JK (2003) *Photochem Photobiol Sci* 2:1018
19. Chun H, Wang Y, Tang H (2001) *Appl Catal B* 30:277
20. Schwarz PF, Turro NJ, Bossmann SH, Braun AM, Wahab AMAA, Durr H (1997) *J Phys Chem B* 101:7127
21. Gomez M, Magnusson E, Olsson E, Hagfeldt A, Lindquist SE, Granqvist CG (2000) *Sol Energy Mat Sol C* 62:259
22. Justicia I, Garcia G, Battiston GA, Gerbasi R, Ager F, Guerra M, Caixach J, Pardo JA, Rivera J, Figueras A (2005) *Electrochim Acta* 50:4605
23. Natarajan C, Fukunaga N, Nogami G (1998) *Thin Solid Films* 322:6
24. Liu GQ, Jin ZG, Liu XX, Wang T, Liu ZF (2007) *J Sol-Gel Sci Technol* 41:49
25. Fukuda H, Matsumoto Y (2005) *Electrochim Acta* 50:5329
26. Karuppuchamy S, Nonomura K, Yoshida T, Sugiura T, Minoura H (2002) *Solid State Ion* 151:19
27. Matsumoto Y, Ishikawa Y, Nishida M, Li S (2000) *J Phys Chem B* 104:4204
28. Peiró AM, Brillas E, Peral J, Domènech X, Ayllón JA (2002) *J Mater Chem* 12:2769
29. Palomares E, Clifford JN, Haque SA, Lutz T, Durrant JR (2003) *J Am Chem Soc* 125:475
30. Fischer R, Fischer E, de Portu G, Roncari E (1995) *J Mater Sci Lett* 14:25
31. Meulenkamp EA (1997) *J Electrochem Soc* 144:1664
32. Lassaletta G, Fernandez A, Esoinos JP, Gonzalez-Elipe AR (1995) *J Phys Chem* 99:1484
33. Hua ZL, Shi JL, Zhang LX, Ruan ML, Yan JN (2002) *Adv Mater* 14:830
34. Somasundaram S, Tacconi N, Chenthamarakshan CR, Rajeshwar K, de Tacconi NR (2005) *J Electroanal Chem* 577:167
35. Wang L, Wang N, Zhu L, Yu H, Tang H (2008) *J Hazard Mater* 152:93
36. Hidaka H, Nagaoka H, Nohara K (1996) *J Photochem Photobiol A* 98:73
37. Sun CC, Chou TC (2000) *J Mol Catal A* 151:133
38. Yang S, Liu Y, Sun C (2006) *Appl Catal A* 301:284
39. Dai K, Chen H, Peng T, Ke D, Yi H (2007) *Chemosphere* 69:1361
40. Siham A, Salman SR (2002) *J Photochem Photobiol A* 148:161